Food Bioprocess Technol
DOI 10.1007/s11947-010-0378-5

ORIGINAL PAPER

Modeling and Simulation of Microwave Heating of Foods Under Different Process Schedules

Laura Analía Campañone · Carlos A. Paola · Rodolfo H. Mascheroni

Received: 24 November 2009 / Accepted: 6 May 2010

Abstract This paper describes the development of a simulation model for heating of foods in microwave ovens and its uses to optimize food heating strategies. The solution of the coupled energy and mass microscopic balances considers the electromagnetic energy absorption as well as temperature-dependent thermal, transport, and dielectric properties. The microscopic balances are highly nonlinear coupled differential equations, which were solved using finite element software (Comsol Multiphysics). Maxwell equations were employed in order to describe the interaction between electromagnetic radiation and food. The mathematical model allowed the evaluation of the effect of product size and composition in the temperature profiles that developed inside the food that was radiated either on one or both sides. In order to improve the nonuniform temperature profiles that occurred within foods under continuous operation, different operation schemes were evaluated: intermittent cycles, joint action of microwaves with air impingement, and the effect of interference of electromagnetic waves.

L. A. Campañone · R. H. Mascheroni
CIDCA (Centro de Investigación y Desarrollo en Criotecnología de Alimentos), CONICET La Plata–UNLP,
calle 47 y 116,
La Plata 1900 Buenos Aires, Argentina

L. A. Campañone · R. H. Mascheroni (✉)
MODIAL, Facultad de Ingeniería,
Universidad Nacional de La Plata,
La Plata, Buenos Aires, Argentina
e-mail: rhmasche@ing.unlp.edu.ar

C. A. Paola
Facultad de Ciencias Astronómicas y Geofísicas,
Universidad Nacional de La Plata,
La Plata, Buenos Aires, Argentina

Published online: 08 June 2010

Keywords Microwave heating · Simulation · Energy balance · Cycles · Convection · Wave interference

Introduction

Microwave heating of foods is an efficient procedure due to its capacity to dissipate energy inside the product through the interaction of radiation with water molecules. Microwaves are utilized for different processes such as baking, thawing, heating, cooking, and drying (Datta & Anantheswaran 2001; Turabi et al. 2008; Sakiyan et al. 2010, Campañone & Zaritzky 2005, 2009; Cha-um et al. 2010). They offer several advantages: reduction of the environmental impact, energy saving when compared to the traditional methods, use of clean energy, spatial saving, and less processing time. Microwave heating either alone or combined with other methods offers these advantages that cannot be obtained by the traditional techniques. Also, it has some disadvantages: low penetration of radiation in bulk products, low energy absorption due to the dielectric properties of some materials and the nonuniform heating of foods that are heterogeneous, have nonuniform composition, geometries, and size ranges, as well as in those foods which dielectric properties drastically change with temperature, i.e., defrosting (Ku et al. 2002; Vadivambal & Jayas 2010).

In order to characterize temperature and moisture distribution during food heating, coupled mass and energy balances must be solved taking into account the absorption of electromagnetic energy. The distribution of the electric and magnetic fields in microwave ovens with or without any load has been described by Maxwell equations (Dibben & Metaxas 1994; Verboven et al. 2003; Rattanadecho 2006). Currently, two ways have been followed to describe the electromagnetic energy distribution inside the foods: to

solve Maxwell equations (Ayappa 1997; Oliveira & Franca 2002; Basak & Kumaran 2005) or to apply Lambert's approximate law which deals with an exponential energy decay inside the product (Tong & Lund 1993; Lin et al. 1995; Chamchong & Datta 1999; Liu et al. 2005).

Ayappa et al. (1991) have compared the power distribution inside the foods as predicted by both laws. They concluded that the difference in the power delivered inside the food per volume unit calculated with the two methods was within 1% when the thickness of the sample was threefold higher than the depth of penetration. Based on the same criterium, Oliveira & Franca (2002) found that the approximate law could be utilized in cylindrical foods when the diameter is sevenfold larger than penetration thickness. Also Yang & Gunasekaran (2004) have compared experimental temperature profiles in agar gel samples of cylindrical geometry with numerical data obtained by Maxwell and Lambert laws, showing that the first ones were more accurate. In this work, Maxwell's equations were selected to describe the microwave heating of foods.

Temperature and humidity distribution during food heating can be obtained by solving the coupled mass and energy balances, taking into account the electromagnetic energy absorption as well as thermal, transport, and dielectric properties which are temperature-dependent. Both balances lead to highly nonlinear coupled differential equations, without analytical solution. Therefore, the equations were solved by implementing numerical simulation. Numerical simulation allows the evaluation of the effect of the particular characteristics of foods (composition, structure, and size) and the operating conditions on temperature profiles and moisture content. Numerical simulation also allows the characterization of the nonuniformity of temperature profiles during heating.

Several technologies associated to microwaves have been proposed with the aim to obtain more uniform temperature profiles. From these, intermittent cycles (on–off) were one of the most utilized because microwaves provide a rapid temperature increase during the "on" periods and then the temperature profiles became more uniform due to internal heat conduction during the "off" periods. Power cycles have been studied in several research works (Chamchong & Datta 1999; Gunasekaran & Yang 2007).

Jet impingement is another method that was proposed in combination with microwaves, creating what is called hybrid ovens (Walker & Li 1993; Datta et al. 2005). Despite the fact that microwaves can rapidly raise the temperature of the foodstuffs, some products show a soggy texture after heating and the lack of surface browning that is typical in convective ovens. In jet impingement ovens, the air removes the water located at the surface and easily produces surface browning in baked foods.

The electromagnetic behavior inside domestic ovens depends on the relationship between the oven size and the size and shape of the product. Several systems dealing with the direct control of product heating have been investigated (Bows et al. 1999; Gerling 2000). To this respect, the interference of electromagnetic waves (IEW) was employed in order to obtain uniform temperature profiles during heating. In IEW, two coherent mutually excluded signals interfere in a constructive way within a special wave guiding system where the signal phases vary one respect the other.

In this work, the aims of this study were:

1. to characterize the temperature distribution within the product by solving the mass and energy microscopic balances, taking into account the electromagnetic interaction with the product
2. to employ the developed model for evaluating the thermal response of foods with different sizes, under different operating conditions, such as radiation over one or both sides, power cycles, use of air convection, and the effect of incident wave interference
3. to determine which of the previous processes is the most effective to improve uniformity in temperature profiles and lessen processing times

Materials and Methods

Mathematical Model

To accurately predict temperature and humidity profiles during food heating, it is necessary to develop a mathematical model that adequately represent the physical system and takes into account the thermal, transport, and dielectric properties of the material under study. The following assumptions were used during the development of this mathematical model:

1. uniform initial temperature and water concentration within the products
2. variable thermal and dielectric properties
3. no volume change during heating
4. plane plate geometry, one dimensional heat and mass transfer
5. convective and evaporative boundary conditions for heat transfer

To describe heat transfer within the food, a microscopic balance of energy is formulated, which includes the internal generation term originated by the energy delivered by microwaves (Ayappa 1997):

$$\rho C_{\mathrm{p}} \frac{\partial T}{\partial t} = \nabla (k_{\mathrm{T}} \nabla T) + Q \tag{1}$$

where ρ, C_{p}, and k_{T} are the density, specific heat, and thermal conductivity of the food, respectively; Q is the

volumetric heat generation term originated by the interaction with microwaves.

The initial and boundary conditions are:

$$t = 0 \qquad T = T_{\text{ini}} \qquad 0 \le x \le L \tag{2}$$

$$t > 0 \qquad -k_{\text{T}} \frac{\partial T}{\partial x} = h(T - T_{\text{a}}) + L_{\text{vap}}\, k'_{\text{m}} \left(C_{\text{w,s}} - C_{\text{equi}}\right)$$
$$x = 0 \qquad \text{and} \qquad x = L \tag{3}$$

where x=0 indicates the food surface, L is the thickness of the product, h is the heat transfer coefficient, T_{a} and T_{ini} are air and food initial temperatures, respectively, L_{vap} is the heat of vaporization of water, k'_{m} is the mass transfer coefficient, $C_{\text{w,s}}$ is water concentration (in food surface), and C_{equi} is the equilibrium water concentration in air.

Equation (3) includes a simplification that is to consider evaporation only at the food surface. This assumption is valid for heating process at low exposition times, when product temperature is maintained below 100 °C and it is not valid for other processes such as oven cooking or microwave drying (Datta 2007). In the present work, it is assumed that weak evaporation occurs and therefore Eq. (3) can be applied. Other authors have used similar boundary condition for simulating the microwave heating process (Tong & Lund 1993; Zhou et al. 1995; Pauli et al. 2007).

To calculate the water concentration profile, the microscopic mass balance is formulated as following (Zhou et al. 1995; Pauli et al. 2007; Marra et al. 2010):

$$\frac{\partial C_{\text{w}}}{\partial t} = \nabla (D_{\text{w}} \nabla C_{\text{w}}) \tag{4}$$

where D_{w} is the effective diffusivity coefficient in the food.

The initial and boundary conditions are:

$$t = 0 \qquad C_{\text{w}} = C_{\text{w,ini}} \qquad 0 \le \times \le L \tag{5}$$

$$t > 0 \qquad -D_{\text{w}} \frac{\partial C}{\partial x} = k'_{\text{m}} \left(C_{\text{w,s}} - C_{\text{equi}}\right)$$
$$x = 0 \qquad \text{and} \qquad x = L \tag{6}$$

The microscopic energy balance is solved knowing the power density delivered by the microwaves as a function of position within the food. To this end, Maxwell equations are written in differential form:

$$\nabla x E = -\frac{\partial B}{\partial t} \tag{7}$$

$$\nabla x H = J + \frac{\partial D}{\partial t} \tag{8}$$

$$\nabla . B = 0 \tag{9}$$

$$\nabla . D = \rho_{\text{c}} \tag{10}$$

where E is the electric field, H is the magnetic field, B is magnetic induction field, D is electric displacement, J is the current density, and ρ_{c} is charge density. Constitutive equations assumed were $J=\sigma E$, $D=\varepsilon E$, and $B=\mu H$, where σ is the electrical conductivity, ε is the dielectric constant, and μ is the magnetic permeability of the food. All these properties depend on the frequency of radiation and on temperature.

Maxwell Eqs. (7)–(10), together with the constitutive equations, allow to calculate the distribution of the electric and magnetic fields along the food product.

Considering time-harmonic electromagnetic fields, $E=\hat{E}\, e^{-\text{i}\omega t}$ and $H=\hat{H}\, e^{-\text{i}\omega t}$ and replacing B and D as a function of H and E, the following equations are obtained:

$$\nabla x \widehat{E} = \text{i}\, \omega \mu\, \widehat{H} \tag{11}$$

$$\nabla x \widehat{H} = (\sigma - \text{i}\, \omega \varepsilon)\, \widehat{E} = -\text{i}\, \omega \varepsilon^* \widehat{E} \tag{12}$$

where ε^* is the complex dielectric constant, which consists of two parts: a real component ε' that represents the ability of the material to store energy and an imaginary part ε'' that accounts for the capacity to dissipate energy.

Equations (11) and (12) are then combined and the following equation is obtained (Ayappa 1997):

$$\nabla \left(E . \frac{\nabla \varepsilon^*}{\varepsilon^*} \right) + \nabla^2 E + k^2 E = 0 \tag{13}$$

The solution of Eq. (13) permits to know the distribution of the electric field inside the food. In the present analysis, the permittivity does not change in the direction of the electric field. Then, the first term in Eq. (13) is null and the following expression is obtained:

$$\nabla^2 E + k^2 E = 0 \tag{14}$$

where k depends on the dielectric properties of the foodstuffs, as follows:

$$k = \alpha + i\beta \tag{15}$$

$$\alpha = \frac{2\pi f}{c} \sqrt{\frac{\varepsilon' \left(\sqrt{(1 + \tan^2 \delta)} + 1 \right)}{2}} \tag{16}$$

$$\beta = \frac{2\pi f}{c}\sqrt{\frac{\varepsilon'\left(\sqrt{(1+\tan^2\delta)}-1\right)}{2}} \tag{17}$$

where f is the frequency of radiation and the loss tangent (tan δ) is calculated using the dielectric properties of the food material:

$$\tan\delta = \frac{\varepsilon''}{\varepsilon'} \tag{18}$$

To know the electric field, Eq. (14) must be solved assuming the following boundary conditions:

$$nx\left(\widehat{E}_1 - \widehat{E}_2\right) = 0 \tag{19}$$

$$nx\left(\widehat{H}_1 - \widehat{H}_2\right) = 0 \tag{20}$$

where the subscript 1 indicates the air medium and the subscript 2 the food. These boundary conditions imply that the tangential components of the electric and magnetic fields are continuous through the boundaries. Eq. (20) can be expressed in function of the electric field through the following relationship:

$$\frac{\partial E}{\partial x} = \mathrm{i}\mu_0\omega H \tag{21}$$

In general, the analytical solution to Eq. (14) can be represented as a combination of waves propagating in opposed directions:

$$E = A_2 e^{\mathrm{ikx}} + B_2 e^{-\mathrm{ikx}} \tag{22}$$

The coefficients A_2 and B_2 in Eq. (22) are complex values that are calculated using boundary conditions (19) and (20), generating a set of linear differential equations that originates a block diagonal matrix. When the food is radiated on one side (left), the intensity of the incident electromagnetic field E_L is known and the following equation system is obtained:

$$\begin{aligned} &E_L + B_1 - A_2 - B_2 = 0 \\ &E_L k_1 - k_1 B_1 - k_2 A_2 + k_2 B_2 = 0 \\ &e^{ik_2 L} A_2 + e^{-ik_2 L} B_2 - e^{ik_1 L} A_1 = 0 \\ &k_2 e^{ik_2 L} A_2 - k_2 e^{-ik_2 L} B_2 - k_1 e^{ik_1 L} A_1 = 0 \end{aligned} \tag{23}$$

The complex coefficients A_2 and B_2 are obtained by solving this system; then the electric field inside the food can be estimated (Eq. 22).

The solution of the electric field for a product radiated on both sides is the result of the superposition of the solution previously obtained, considering that both opposite faces are radiated with an external electric field of the same module and phase.

The IEW was also analyzed in this work for a plate radiated on both sides by electromagnetic waves of the same strength and phase shifting. It must be noted that phase shifting means a change on the total length from the source to the food core. The model takes into account this case, through the following functionality for the electric fields within the food:

$$E_\mathrm{L} = A_2 e^{\mathrm{ikx}} + B_2 e^{-\mathrm{ikx}} \tag{24}$$

$$E_\mathrm{R} = A_2 e^{\mathrm{i(kx+\phi)}} + B_2 e^{-\mathrm{i(kx+\phi)}} \tag{25}$$

where φ is the shift angle of the incident waves, and A_2 and B_2 are the constants resulting from the solution of equation (14) when considering the boundary conditions (19) and (21). The electric field inside the food arises from the addition of both solutions.

Once the electric field is known, the density of energy can be calculated by applying the Poynting's theorem:

$$Q = \frac{1}{2}\omega\varepsilon_\circ\varepsilon'' E.E^* \tag{26}$$

where ε_o is the permittivity of vacuum and E^* is the complex conjugate of the electric field.

Microscopic balances of energy (Eq. 1) and mass (Eq. 4) are coupled, and together with their boundary conditions, they form a system of nonlinear partial differential equations. A commercial finite element software Comsol Multiphysics version 3.2 was used (Comsol Inc., Burlington, MA, USA) to solve the equations. The software was able to converge with a relatively coarse mesh of 240 nodes. The time dependent solver was used and the direct UMFPACK linear system solver was employed. The calculations took a few seconds to reach to the final time of the process with the direct solver. The solution of Eq. (14) was programmed using Matlab 6.5 (Mathworks, USA). The developed code evaluates—at each time step—the dielectric properties as a function of temperatures predicted by the previous step and then it calculates the distribution of the electric field inside the food. The values of electric field at each food position were utilized to calculate the energy density delivered to the food (Eq. 26) and then this value was supplied to the Comsol software to predict temperature and mass profiles at the next time step.

Results and Discussion

Validation of the Mathematical Model

The model was validated with experimental temperature data from literature for the microwave heating of foods and analogues.

Radiated on Both Sides First, numerical predictions were validated with temperature data of thick samples radiated on both sides. This situation was analyzed using the experimental data reported by Van Remmen et al. (1996). The product studied was agar gel with different compositions: 2% agar (*w*/*w*), 2% agar +30% (*w*/*w*) starch, and 2% agar +3% NaCl (*w*/*w*). In all cases, samples were 8 cm thickness, and they were radiated on both sides (E=3,000 V/m, initial sample temperature=18 °C). Table 1 shows the thermal and dielectric properties used in the mathematical model.

Figure 1a shows the predicted power density as a function of the food internal position. A wavy pattern can be observed, particularly in agar gel and its combination with starch (penetration values of 2.6 cm and 2.5 cm, respectively). However, when salt was added, the samples exhibited a decreasing exponential behavior similar to that predicted by Lambert's law. This is the result of a marked increase in the dielectric loss factor after the salt addition, with the consequent penetration decrease (agar+salt penetration=0.98 cm) and an increase in attenuation factor. Under these conditions, the food shows a dominant skin effect.

Values of the power density were used in the energy balance to predict temperature profiles. Figure 1b, c, and d shows the numerical and experimental values after heating for 90 s. The model follows the behavior and trend of the experimental data. The larger difference was noted in the agar+salt samples. Such a difference may be due to the use of constant dielectric properties available in literature and also to the use of the same thermal properties for gels with a different composition.

In order to validate this mathematical model in smaller products radiated on both sides, experimental data for the heating of bread samples were employed (Tong & Lund 1993). The thermal, dielectric, and moisture diffusion properties used in the model are shown in Table 1, as a function of temperature (T) and moisture content (m). The sample was heated from T_{ini}=25 °C and radiated in an electric field with two different amplitudes of 2,830 and 4,250 V/m. Figure 2a shows the calculated values of the power density for both amplitude values. Minor values were detected on the surface whereas the major ones were found in the center of the plate, due to the interaction of incident waves inside the foods.

Values in Fig. 2a were used to predict temperature profiles. Figure 2b and c shows the predictions for the center of the sample and a position near to the surface (7/8 half thickness) when using an electric field of 2,830 V/m. Predictions for the surface in the field of higher amplitude are displayed in Fig. 2d. Only predicted values lower than 100 °C are shown, that is the temperature range for which the present mathematical model was developed.

Radiated on One Side This model was also utilized to predict temperature values in products radiated on one side. First the model was tested with experimental temperature data obtained in hamburgers of 11 cm diameter and 1.3 cm height with different fat contents (Gunasekaran 2002). Dielectric properties depending on fat content (G), of samples were used for the model (Table 1). Hamburgers were heated from T_{ini}=10 °C under the following heating conditions: E=6,925 V/m, h=11.3 W/(m^2 °C), and T_a=20 °C. Figure 3a shows the predicted values of power density. The behavior was found to be strongly oscillatory, showing a minimum and a maximum value of absorption inside the food. It was also found that the fat content affects the power profiles. At a greater fat content, a higher power density was predicted.

Figure 3b, c, and d shows predicted and experimental values of temperature obtained for hamburger surface. This model simulates adequately experimental temperature values

Table 1 Thermal, transport, and electromagnetic properties of different products

Property	Agar	Agar+starch	Agar+salt	Bread	Meat
Density (kg/m^3)	1,000 (f)	1,000 (f)	1,000 (f)	152 (c)	1,053 (g)
Thermal conductivity (W/(m°C))	0.6 (f)	0.6 (f)	0.6 (f)	$\ln k_T = 6.03 - 17.7m - 0.061T + +0.065mT + 10^{-4}T^2, T(K)$ (c)	$0.457 + 3.74\ 10^{-4}T$ (g)
Specific heat (J/(kg°C))	4,200 (f)	4,200 (f)	4,200 (f)	$(1-m)Cp_{solid} + mCp_{water}$; $Cp_{solid} = 10^3(0.098 + 0.0049T)$ $T(K)$ (c)	3,474.86 (g)
Dielectric constant (dimensionless)	73.6 (a)	56 (f)	75 (b)	5.4 (d)	$50.69 - 0.008T + 5\ 10^{-4}T^2 - - 1.21G + 0.03G^2$ (h)
Dielectric loss factor (dimensionless)	11.50 (a)	9 (f)	35 (b)	0.75 (d)	$16.7 - 0.05T + 7\ 10^{-4}T^2 - 0.22$ (h)
Diffusion coefficient (m^2/s)	–	–	–	$2.5 10^{-9}$ (e)	$2 10^{-12}$T$-1 10^{-12}$ (i)

a Padua (1993), *b* Sakai et al. (2005), *c* Christenson et al. (1989), *d* Ayappa et al. (1991), *e* Tong & Lund (1990), *f* Van Remmen et al. (1996), *g* Campañone et al. (2001), *h* Gunasekaran & Yang (2007), *i* Merts et al. (1998)

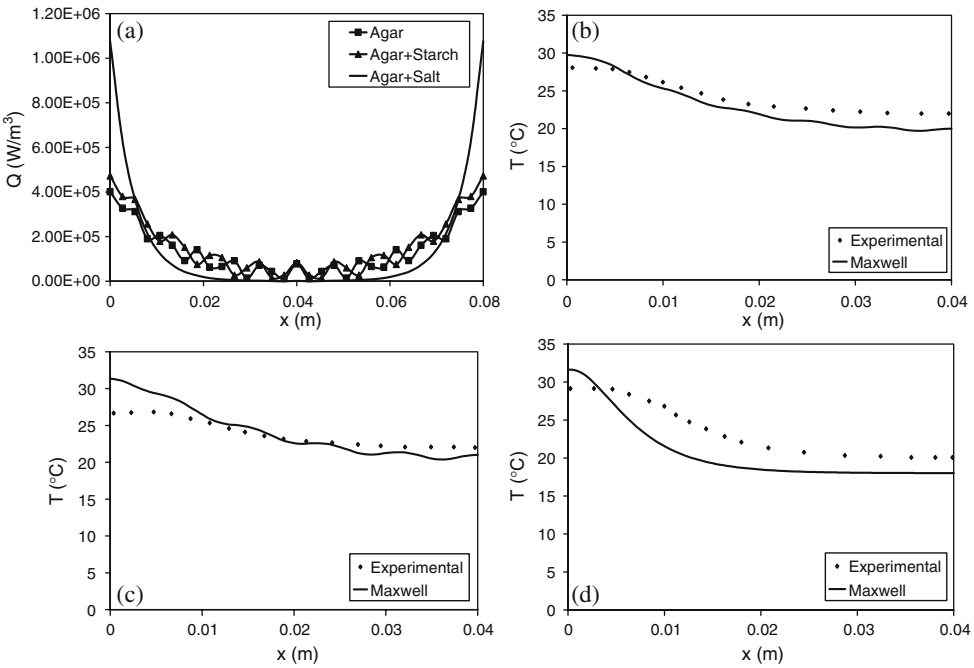

Fig. 1 **a** Predicted power density on an agar gel slab with different compositions. **b**, **c**, **d** Experimental (Van Remmen et al. 1996) and predicted (present model) temperature profiles on agar slabs with different compositions after 90 s heating

for this size (1.3 cm) and different dielectric properties (due to the different fat contents of the hamburgers).

Finally, the mathematical model was validated by using experimental temperature data of agar gel slabs of 3 or 0.9 cm thickness (Barringer et al. 1995). Dielectric and thermal properties used in this model are presented in Table 1. The samples were heated from T_{ini}=4 °C under the following heating conditions: E=3,500 V/m and h=4 W/(m^2 °C). Figure 4a and b shows the predicted values of power density. Figure 4c and d presents predicted and experimental temperature values after 7 min of heating. It can be seen that the model follows the trend of experimental values for both product sizes.

In brief, this model is applicable to describe microwave heating as it allows temperature prediction for products of different sizes within a wide range of dielectric properties and electric field amplitudes.

Effect of Product Size on Temperature Profiles

Once the model was validated, it was used to predict humidity and temperature profiles in meat products.

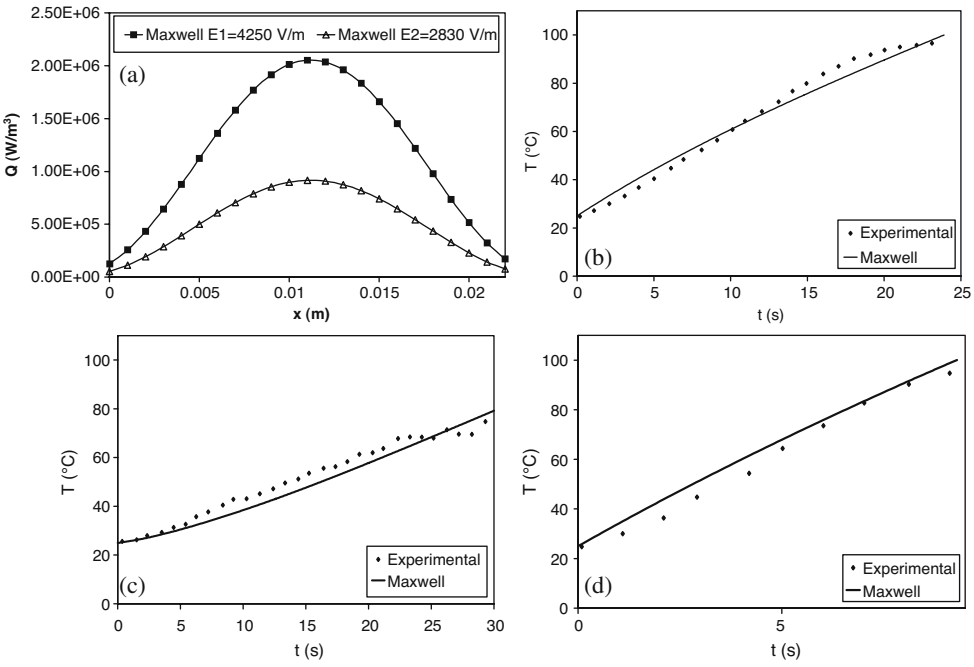

Fig. 2 **a** Predicted power density in a bread sample radiated on both sides. **b**, **c**, **d** Predicted (present work) and experimental (Tong and Lund 1993) temperature values for a bread sample as a function of heating time

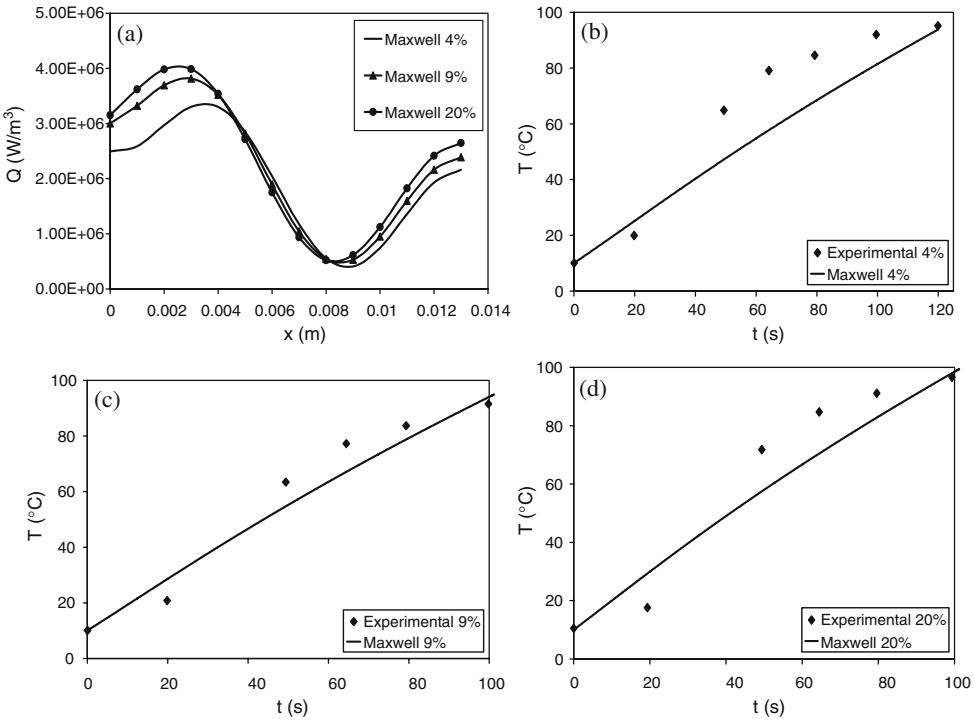

Fig. 3 **a** Predicted power density distribution inside hamburger samples with different fat contents. **b**, **c**, **d** Predicted (*lines*, this work) and experimental (Gunasekaran 2002) surface temperature of hamburger with different fat contents

Thermal, transport, and electromagnetic properties used in calculations are reported in Table 1. The following input parameters were used: heating with an electric field of 6,000 V/m, an air temperature of 25 °C, a heat transfer coefficient of 5 W/(m^2 °C), and the initial conditions T_{ini}= 10 °C and C_{ini}=779.22 kg/m^3. Radiation time was 1 min, unless otherwise indicated.

The model was solved by taking into account that the product could be radiated on one or both sides. First, the behavior of those products that radiated only on one side was analyzed.

Figure 5a–b shows the results corresponding to power density, obtained by Maxwell's equations as a function of product size, whereas Fig. 5c–d shows the corresponding

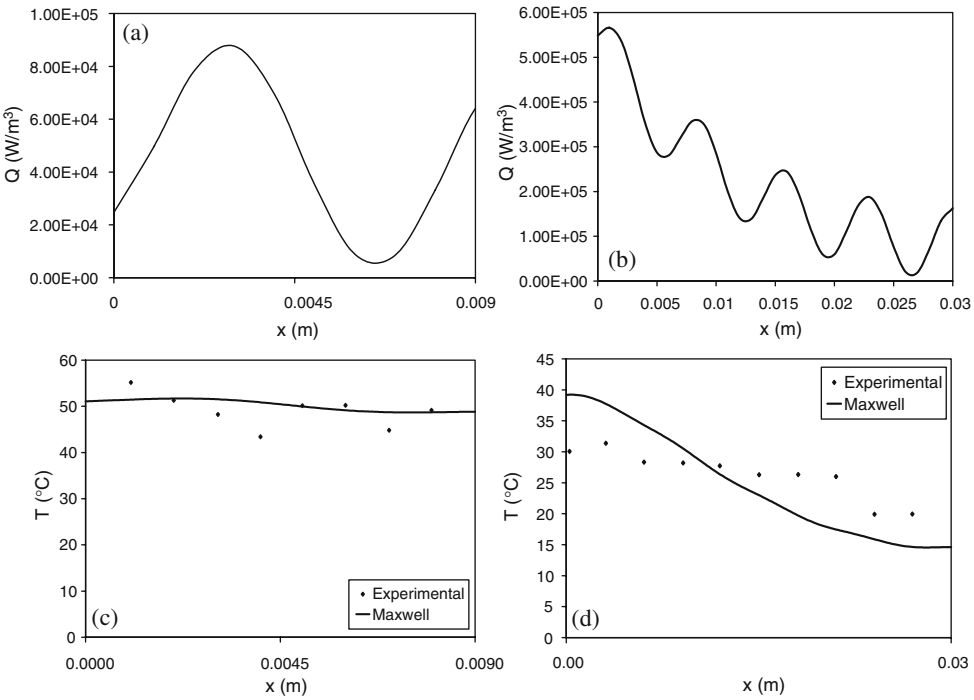

Fig. 4 Predicted power density for agar gel samples of: **a** 0.9 and **b** 3.0 cm. **c**, **d** Predicted temperature (*lines*, this work) vs experimental data (Barringer et al. 1995) on agar gel slabs radiated on one side for 7 min

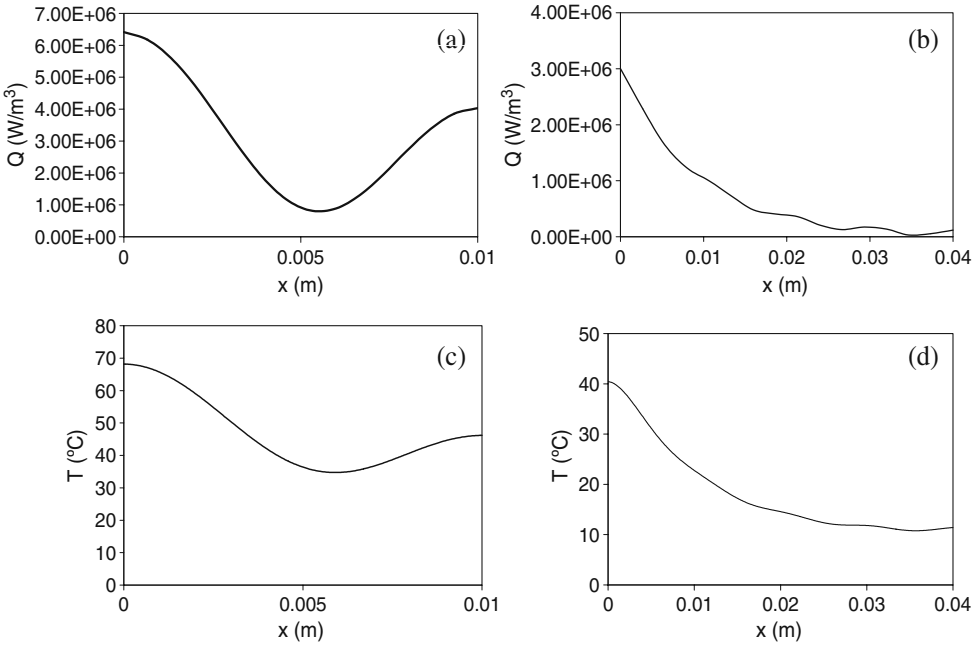

Fig. 5 Power density as a function of the slab size: **a** 1 and **b** 4 cm. **c**, **d** Temperature profiles as a function of the slab size radiated on one side

temperature profiles. In each case, the humidity profiles were also calculated (data not shown). It was found that in small products the electric field within the food and the absorbed power present a highly wavy behavior. For larger products the predicted behavior tends to follow Lambert's law. In the analyzed case, the critical value was approximately 4 cm, which was coincident with the critical value predicted by Ayappa et al. (1991) for the application of Lambert's law in the heating of meat products. Below the critical size, the obtained profiles are not uniform, the surface becomes the hottest point, and there are other internal points in which the electromagnetic energy absorption increases. Humidity profiles did not present a wavy pattern (data not shown) due to the poor dependence of water diffusion coefficient with temperature and short exposure to radiation (1 min).

The mathematical model was also used to predict the behavior of products radiated on both sides. Figure 6a–d shows the results obtained for power density and temperature profiles in foods of different sizes. It was supposed

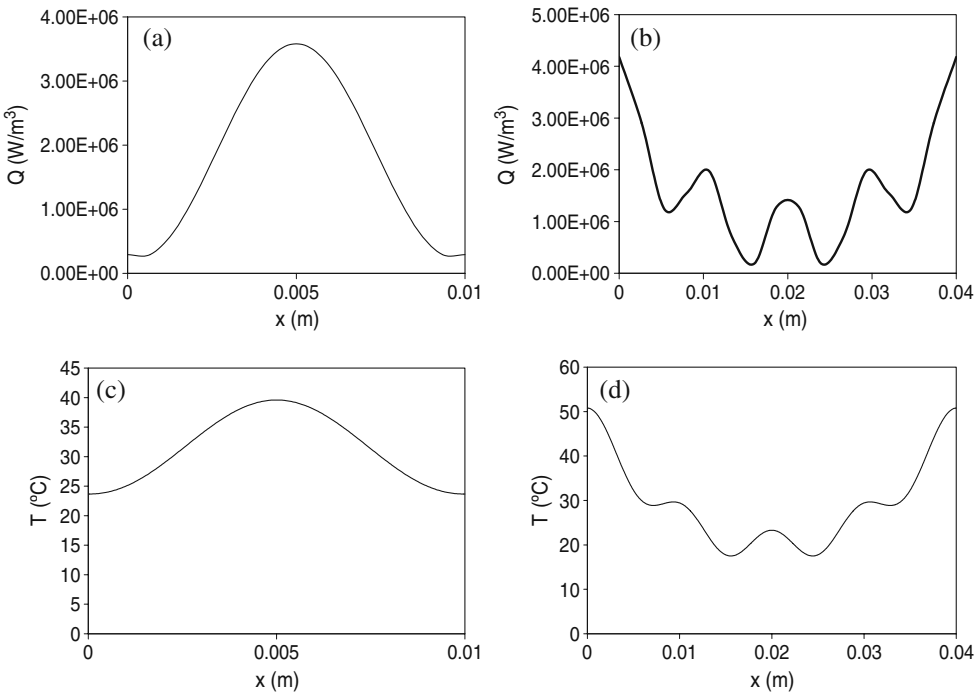

Fig. 6 Power density as a function of the slab size: **a** 1 and **b** 4 cm. **c**, **d** Temperature profiles obtained as a function of the slab size radiated on both sides

that the radiation on both sides was carried out by "in phase" electromagnetic waves of the same intensity. An undulating response pattern of energy absorption was observed within the product: an absorption peak in the center and at each 1 cm from the center of the slab. Temperature profiles showed a symmetric oscillatory shape following that of the power density. In plates that radiated on both sides, the critical value from which Lambert's law was valid was found to be greater than 4 cm.

The interaction of waves inside the food as a function of the thickness for food slabs radiated on both sides is an important fact to be taken into account. Figure 7 shows the power per volume unit in the food center as a function of food thickness. The effect of thickness on power density creates a wavy curve whose value rapidly decreases with the decrease in thickness. This effect can be attributed to the effect of the superposition of the principal waves (those incidents on opposite faces) with their own internal reflections. The amplitude is depending on food thickness because the phase shift between incident and reflected waves can intensify or attenuate the maximum in the central point. The interference between incident waves and the first reflection will be constructive when the phase difference between waves is $2n\pi$, n being an integer number. In our model, this phase difference is the food thickness (L). The number of wavelengths through the thickness is $2\pi L/\lambda_m$, λ_m being the wavelength in the medium. Then, the constructive interaction occurs when the thickness of the slab is $L=n\ \lambda_m$. This phenomenon is of utmost importance because the decrease of the heating time strongly depends of the fulfillment of the previous relation. This is a specific characteristic in microwave heating that cannot be observed in traditional convective heating.

Use of Alternative Heating Methods to Obtain More Uniform Temperature Profiles

The mathematical model can be used to predict the behavior of foods as a function of the operating conditions under MW, convective or combined heating.

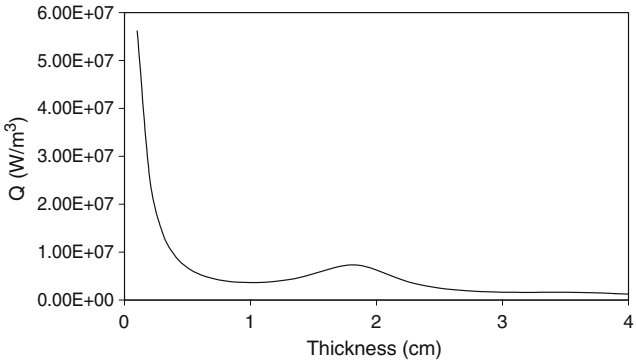

Fig. 7 Power density absorbed in the center of the meat slab as a function of its size

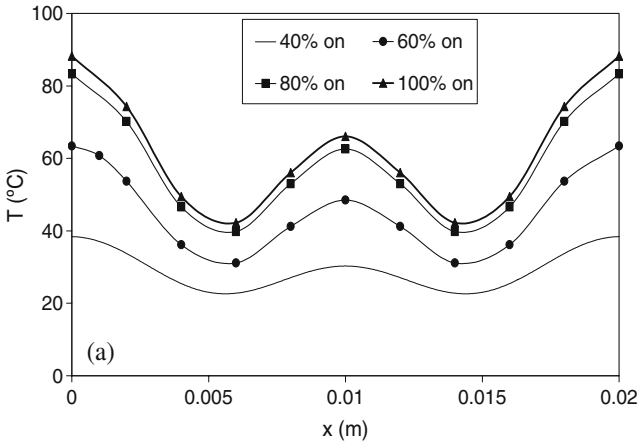

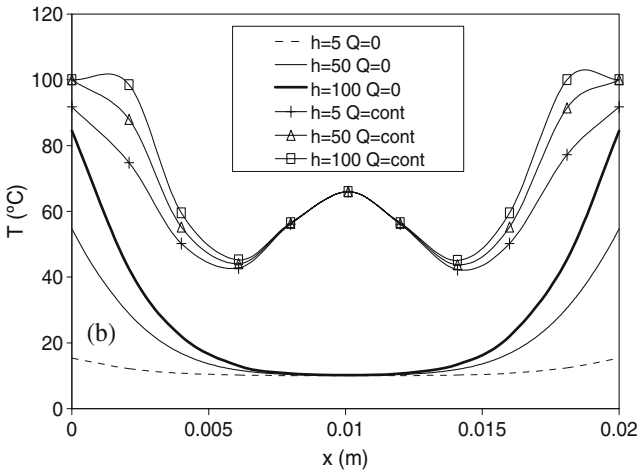

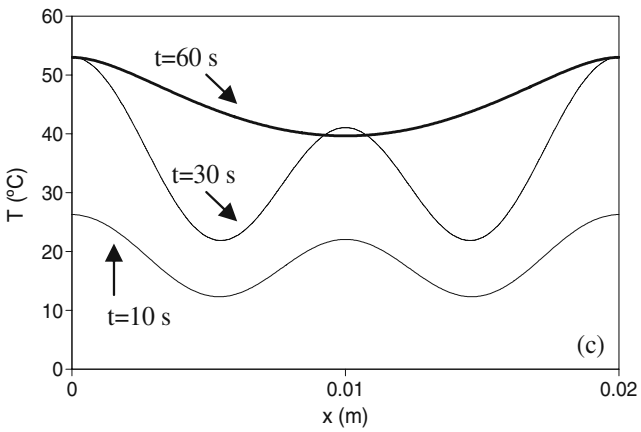

Fig. 8 **a** Temperature profiles obtained for different power cycles. **b** Temperature profiles obtained combining microwaves and air convection (Q=continuous) and traditional heating without microwaves (Q=0). **c** Temperature profiles predicted for a slab radiated on both sides for 30 s in phase and 30 s π radians phase-shifted with respect to the other

Heating under optimal operating conditions was the main objective in these simulations: to minimize nonuniformity in temperature profiles without increasing weight loss.

All the studies were performed by simulating the heating of a meat slab with a thickness of 2 cm.

Intermittent Cycles of Power (ON–OFF)

Ovens can work in a continuous or intermittent way (power cycles ON–OFF). The model was employed to analyze the effect of these cycles in the nonuniformity of temperature profiles. Nonuniformity of these profiles was calculated as a standard deviation with respect to the average temperature. To model the intermittent on–off cycles in a simple operation, the magnetron is considered "on" at full power for some time during the cycle (indicated by a percentage of the total time) and "off" during the rest of the time. Heating periods of 10 s during 1 min of total operation were considered.

Figure 8a shows the effect of different power cycles on a slab radiated on both sides. Similar results were predicted on slabs radiated on one side. It is clearly demonstrated that the temperature increases as the fraction of "true" heating time increases. On the other hand, when increasing the time that the magnetron was turned off, the uniformity of the temperature profiles was enhanced at the expense of a longer heating time.

Microwave Heating Combined with Air Convection

Microwaves can rapidly increase the temperature in foods inducing a quick movement of the moisture towards the product surface. If the ambient air is unable to remove it, then it leads to changes in the appearance and attributes, such as a gummy texture in bakery foods. For this reason, microwaves are combined with other systems as infrared heating or jet impingement of hot air to facilitate the removal of surface humidity.

Several possible operating strategies were simulated. The operation was evaluated using three different values of heat transfer coefficients: 5 (without air circulation), 50, and 100 W/(m^2°C) and air temperature 200 °C (Datta et al. 2005). The mass transfer coefficients were calculated by analogy to those of heat transfer and were found to be in agreement with those reported by other authors (Datta et al. 2005; Erdogdu et al. 2005).

Figure 8b shows the temperature profiles obtained after 1 min of heating under different operating conditions. When food is heated by hot air convection, the surface is the critical point and its temperature raises while the central zone remains at its initial condition. Microwave heating produces a nonuniform final temperature profile, with hot spots located at the center, together with others at the surface. The use of hot air convection coupled to microwaves permits to reach a rapid temperature increase in the product with a more uniform profile.

Interference of the Electromagnetic Waves

The aim of the use of interference of the IEW is to produce changes in the developed temperature profiles. When radiation is applied "in phase," peaks and valleys appear inside the food (as shown in previous sections). By changing the phase of one wave with respect to the other, the hot and cold spots change their position, and this in turn can improve the temperature uniformity.

We simulated the behavior of food heated according to this strategy, with a phase shift of π (180°). The incident waves were of the same intensity E=6000 V/m, in phase during the first 30 s of heating and with a shifted phase for the remaining 30 s. This procedure in now is under experimental study at our laboratory. Figure 8c displays

Table 2 Predicted standard deviation and heating times for different simulated heating schedules

Run	Simulated operating conditions	Standard deviation after 1 min heating (°C)	Time to 100ºC on the surface (s)
C1–C7	ON–OFF cycles	4.94 (40% on), 7.34 (50% on), 10.31 (60% on), 12.96 (70% on), 14.00 (80% on), 14.52 (90% on), 14.62 (100% on)	403 (40% on), 125 (50% on), 114 (60% on), 81 (70% on), 76 (80% on), 72 (90% on), 72 (100% on)
C8	Combined hot air–Mw heating h=5; Q=0; Ta=200ºC	1.48	6201
C9	Combined hot air–Mw heating h=50; Q=0; Ta=200ºC	12.22	414
C10	Combined hot air–Mw heating h=100; Q=0; Ta=200ºC	21.21	110
C11	Combined hot air–Mw heating h=5; Q=continuous; Ta=200ºC	15.67	68
C12	Combined hot air–Mw heating h=50; Q=continuous; Ta=200ºC	22.99	43
C13	Combined hot air–Mw heating h=100; Q=continuous; Ta=200ºC	28.77	28
C14	Interference of EM waves (IEW) 30/30	3.59	180

the temperature profiles on a slab heated for 1 min. A very uniform final temperature profile was observed, suggesting that this method could be effective for flattening the resulting temperature profiles.

Comparison Between the Different Techniques of Operation Simulated

The comparison between the available techniques for MW heating was performed on the basis of two parameters: predicted processing time and nonuniformity of temperature profiles.

To compare heating times, the time needed for meat products to reach 100 °C on the surface was used. Nonuniformity in temperature profiles was compared using the standard deviation with respect to the average temperature after 1 min of heating under the different regimes.

Table 2 shows the heating schedules and the predicted parameters for 14 different simulated heating runs (C1–C14). As can be seen in Table 2, the microwave plus air impingement technique drastically shortened processing times (run C13) at the expense of a very nonuniform temperature profile. On the contrary, interference of the incident waves was found to be the best to achieve uniformity in the temperature profiles (run C14) with a reasonable increase in heating time.

To design the most adequate heating policy for a determined product, these thermal histories must be complemented with experimental or theoretical studies related to food structure (crusting, browning, puffing) or chemical or physical changes (weight loss, color changes, taste, nutrient losses).

Conclusions

This paper describes the development of a simulation model for heating of foods in microwave ovens and uses the developed simulation model to optimize food heating strategies. By using numerical simulation, the following conclusions were obtained:

- When the product within certain size ranges was radiated on both faces, peaks and valleys appeared in the temperature profiles due to the interference of stationary waves.
- Under certain heating strategies and food sizes, the predicted power density distribution was strongly nonuniform.
- The simulation model was used to evaluate intermittent operation. On–off power cycles facilitate uniformity in temperature profiles.
- The simulation model was also used to evaluate microwave heating combined with air impingement. The use of air convection together with microwaves significantly reduces the processing time.
- Finally, the use of incident wave interference was found to be an efficient strategy to produce uniform temperature profiles.

Acknowledgments The financial support given by the University of La Plata, Consejo Nacional de Investigaciones Científicas y Técnicas (CONICET) and Agencia Nacional de Promoción Científica y Tecnológica (ANPCyT) from Argentina is gratefully acknowledged.

References

Ayappa, K. G., Davis, H. T., Crapiste, G., Davis, E. A., & Gordon, J. (1991). Microwave heating: an evaluation of power formulations. *Chemical Engineering Science, 46*(4), 1005–1016.

Ayappa, K. G. (1997). Modelling transport processes during microwave heating: a review. *Reviews in Chemical Engineering, 13*(2), 1–67.

Barringer, S. A., Davis, E. A., Gordon, J., Ayappa, K. G., & Davis, H. T. (1995). Microwave heating temperature profiles for thin slabs compared to Maxwell and Lambert´s law predictions. *Journal of Food Science, 60*(5), 1137–1142.

Basak, T., & Kumaran, S. S. (2005). A generalized analysis on material invariant characteristics for microwave heating of slabs. *Chemical Engineering Science, 60*, 5480–5498.

Bows, J. R., Patrick, M. L., Janes, R., Metaxas, A. C., & Dibben, D. C. (1999). Microwave phase control heating. *International Journal of Food Science & Technology, 34*, 295–304.

Campañone, L. A., Salvadori, V. O., & Mascheroni, R. H. (2001). Weight loss during freezing and storage of unpackaged foods. *Journal of Food Engineering, 47*, 69–79.

Campañone, L. A., & Zaritzky, N. E. (2005). Mathematical analysis of microwave heating process. *Journal of Food Engineering, 69*, 359–368.

Campañone, L. A., & Zaritzky, N. E. (2009). Mathematical Modeling and simulation of microwave thawing of large solid foods under different operating conditions. *Food And Bioprocess Technology*. doi:10.1007/s11947-009-0249-0.

Chamchong, M., & Datta, A. K. (1999). Thawing of foods in a microwave oven: I. Effect of power levels and power cycling. *The Journal of Microwave Power and Electromagnetic Energy, 34*(1), 9–21.

Cha-um, W., Rattanadecho, P. & Pakdee, W. (2010). Experimental and numerical analysis of microwave heating of water and oil using a rectangular wave guide: influence of sample sizes, positions, and microwave power. *Food Bioprocess Technology*, doi:10.1007/s11947-009-0187, in press.

Christenson, M. E., Tong, C. H., & Lund, D. B. (1989). Physical properties of baked products as functions of moisture and temperature. *Journal of Food Processing and Preservation, 13*, 201–217.

Datta, A. K., & Anantheswaran, R. C. (2001). *Handbook of microwave technology for food applications*. USA: Marcel Dekker Inc.

Datta, A. K., Geedipalli, S. S. R., & Almeida, M. F. (2005). Microwave combination heating. *Food Technology, 59*(1), 36–40.

Datta, A. K. (2007). Porous media approaches to studying simultaneous heat and mass transfer in food processes. I: problem formulations. *Journal of Food Engineering, 80*, 80–95.

Dibben, D. C., & Metaxas, A. C. (1994). Experimental verification of a finite element solution to heating problems in a multi-mode

cavity. *The Journal of Microwave Power and Electromagnetic Energy, 29*(4), 242–251.

Erdogdu, F., Sarkar, A., & Singh, R. P. (2005). Mathematical modeling of air-impingement cooling of finite slab shaped objects and effect of spatial variation of heat transfer coefficient. *Journal of Food Engineering, 71*, 287–294.

Gerling, J.F. (2000). *Waveguide components and configurations for optimal performance in microwave heating systems*. Gerling Applied Engineering Inc., 1–8.

Gunasekaran, N. (2002). *Effect of fat content and food type on heat transfer during microwave heating*. MS Thesis: Virginia Polytechnic Institute and State University, Virginia, USA.

Gunasekaran, S., & Yang, H. (2007). Effect of experimental parameters on temperature distribution during continuous and pulsed microwave heating. *Journal of Food Engineering, 78*, 1452–1456.

Ku, H. S., Siores, E., Taube, A., & Ball, J. A. R. (2002). Productivity improvement through the use of industrial microwave technologies. *Computers & Industrial Engineering, 42*, 281–290.

Lin, Y. E., Anantheswaran, R. C., & Puri, V. M. (1995). Finite element analysis of microwave heating of solid foods. *Journal of Food Engineering, 25*, 85–112.

Liu, C. M., Wang, Q. Z., & Sakai, N. (2005). Power and temperature distribution during microwave thawing, simulated by using Maxwell's equations and Lambert's law. *International Journal of Food Science & Technology, 40*, 9–21.

Marra, F., De Bonis, M. V., & Ruocco, G. (2010). Combined microwaves and convection heating: a conjugate approach. *Journal of Food Engineering, 97*, 31–39. doi:10.1016/j.jfoodeng.2009.09.012.

Merts, I., Lovatt, S. J., & Lawson, C. R. (1998). *Diffusivity of moisture in whole muscle meat measures by a drying curve method. Proceedings of international congress on advances in the refrigeration systems, food technologies and cold chain* (pp. 473–479). Bulgaria: Sofia.

Oliveira, M. E. C., & Franca, A. S. (2002). Microwave heating of foodstuffs. *Journal of Food Engineering, 53*, 347–359.

Padua, G. W. (1993). Microwave heating of agar gels containing sucrose. *Journal of Food Science, 58*(60), 1426–1428.

Pauli, M., Kayser T., Adamiuk, G., & Wiesbeck, W. (2007). *Modeling of mutual coupling between electromagnetic and thermal fields in microwave heating*. IEEE, 1983–1986.

Rattanadecho, P. (2006). The simulation of microwave heating of wood using a rectangular wave guide: influence of frequency and sample size. *Chemical Engineering Science, 61*, 4798–4811.

Sakai, N., Mao, W., Koshima, Y., & Watanabe, M. (2005). A method for developing model food system in microwave heating studies. *Journal of Food Engineering, 66*(4), 525–531.

Sakiyan, O., Sumnu, G., Sahin, S., Meda, V., Koksel, H. & Chang, P. (2010). A study on degree of starch gelatinization in cakes baked in three different ovens. *Food Bioprocess Technology*, doi:10.1007/s11947-009-0210-2, in press.

Tong, C. H., & Lund, D. B. (1990). Effective moisture diffusivity in porous materials as a function of temperature and moisture content. *Biotechnology Progress, 6*, 67–75.

Tong, C. H., & Lund, D. B. (1993). Microwave heating of baked dough products with simultaneous heat and moisture transfer. *Journal of Food Engineering, 19*, 319–339.

Turabi, E., Sumnu, G., & Sahin, S. (2008). Optimization of baking of rice cakes in infrared–microwave combination oven by response surface methodology. *Food Bioprocess Technology, 1*, 64–73.

Vadivambal, R. & Jayas, D.S. (2010). Non-uniform temperature distribution during microwave heating of food materials—a review. *Food Bioprocess Technology, 2*, 161–171. doi:10.1007/s11947-008-0136-0.

Van Remmen, H. H. J., Ponne, C. T., Nijhuis, H. H., Bartels, P. V., & Kerkhof, P. J. A. M. (1996). Microwave heating distributions in slabs, spheres and cylinders with relation to food processing. *Journal of Food Science, 61*(6), 1105–1117.

Verboven, P., Datta, A. K., Anh, N. T., Scheerlinck, N., & Nicolai, B. M. (2003). Computation of airflow effects on heat and mass transfer in a microwave oven. *Journal of Food Engineering, 59*, 181–190.

Walker, C. E., & Li, A. (1993). Impingement oven technology-part III. Combining impingement with microwave (hybrid oven). *Research Department Technical Bulletin, 15*(9), 1–6.

Yang, H. W., & Gunasekaran, S. (2004). Comparison of temperature distribution in model food cylinders based on Maxwell's equations and Lambert's law during pulsed microwave heating. *Journal of Food Engineering, 64*, 445–453.

Zhou, L., Puri, V. M., Anantheswaran, R. C., & Yeh, G. (1995). Finite element modelling of heat and mass transfer in food materials during microwave heating-model, development and validation. *Journal of Food Engineering, 25*, 509–529.